Comparison of Mechanisms for Cavity Growth by Athermal and Thermal Processes

B.B. Glasgow and W.G. Wolfer

September 1983

UWFDM-544

Presented at the Third Topical Meeting on Fusion Reactor Materials, Albuquerque, NM, 19-23 September 1983.

FUSION TECHNOLOGY INSTITUTE

UNIVERSITY OF WISCONSIN

MADISON WISCONSIN

Comparison of Mechanisms for Cavity Growth by Athermal and Thermal Processes

B.B. Glasgow and W.G. Wolfer

Fusion Technology Institute
University of Wisconsin
1500 Engineering Drive
Madison, WI 53706

http://fti.neep.wisc.edu

September 1983

UWFDM-544

Presented at the Third Topical Meeting on Fusion Reactor Materials, Albuquerque, NM, 19-23 September 1983.

COMPARISON OF MECHANISMS FOR CAVITY GROWTH BY ATHERMAL AND THERMAL PROCESSES*

B.B. GLASGOW and W.G. WOLFER

Fusion Engineering Program, Nuclear Engineering Department, University of Wisconsin, Madison, Wisconsin 53706

The energy expended per metal atom removed from an overpressurized bubble is evaluated for three bubble growth mechanisms under constant helium generation or implantation rates. These mechanisms are self-interstitial expulsion, loop punching, and thermal vacancy absorption. It is found that the predominance of each one of the three mechanisms depends strongly on the bubble size, the temperature and the helium generation rate.

1. INTRODUCTION

The energy required to place a helium atom interstitially into a metal is substantial. Pseudopotential calculations[1] for helium in aluminum indicate an energy of 2.69 eV, whereas computer simulation[2] of Cu and W gave values of 1.97 eV and 5.44 eV, respectively, for the helium interstitial formation energy, E^f_{He}. For interstitial helium in Ni, Wilson and Johnson[3] obtained an energy of about 4.5 eV, and for bcc Fe an energy of 5.4 eV. These energies are comparable to the formation energy E^f_I of a self-interstitial, but less than the formation energy of a Frenkel pair. As a result of these large energies for helium interstitials, helium produced by (n,α) reactions or implanted tends to precipitate and form helium inclusions or bubbles.

Various mechanisms for the growth of helium clusters and bubbles have been proposed. From computer simulation studies of helium-vacancy clusters, Wilson and coworkers[4,5] found that 5 helium atoms can be trapped in one vacancy. Trapping of an additional helium atom causes the emission of a self-interstitial which remains, however, attached to the cluster. This athermal growth of helium clusters into bubbles was further investigated with a rate-theory model by Baskes et al.[6] They concluded that the athermal emission of self-interstitials by bubbles which trap more helium atoms can indeed provide an explanation for the formation of the high density of bubbles which precedes blistering at low temperatures. In all these theoretical studies, effects due to lattice vibrations were not considered; in essence, the results are strictly valid for 0 K only. In addition, rather small helium-vacancy clusters were modeled containing only a few helium atoms and vacancies. The transition to larger bubbles therefore requires further investigation. Evans[7] has proposed that the overpressure in helium bubbles is relieved by punching of interstitial-type loops as first suggested by Greenwood, Forman and Rimmer.[8] Again, this is an athermal mechanism of bubble growth. Finally, it is well known that at elevated temperatures above ~ 0.5 T_m, helium bubbles may grow by the absorption of thermal vacancies.

In the present paper we investigate further the above mentioned mechanisms for helium cluster growth, i.e. interstitial emission, loop punching, and thermal vacancy absorption.

*Supported by the Office of Fusion Energy, U.S. Department of Energy, under contract DE-AC02-82ER50282 with the University of Wisconsin.

The purpose of the investigation is threefold. First, we would like to include the effect of temperature for two mechanisms, namely self-interstitial emission and thermal vacancy absorption. Second, we want to find which of these mechanisms is the predominant one for a given temperature, a given helium concentration, and for a given microstructure to be defined below. Third, we wish to extend previous investigations restricted to small helium clusters to larger clusters and bubbles as seen in electron-microscopy studies.

2. SELF-INTERSTITIAL EMISSION

Before analyzing the process of self-interstitial emission by overpressurized bubbles it is first necessary to investigate the possibility that helium atoms are emitted interstitially rather than metal atoms. For the former process, the chemical potential μ_g of helium in the gas phase is equal to the chemical potential of helium interstitials, or

$$C^o_{He} = \exp\{-(E^f_{He} + U_{He} - \mu_g)/kT\} \qquad (1)$$

where C^o_{He} is the helium interstitial concentration, and E^f_{He} its formation energy in a stress-free solid. When a self-interstitial is emitted by the bubble, the Helmholtz free energy of the gas changes by $-\int p\, dV$ where the bubble volume expands from V to V + Ω; Ω is the atomic volume of the host metal. If we neglect the reduction in gas pressure as the bubble volume increases by Ω, the change in the free energy is $-p\Omega = -kTz(y_o)\Omega/\Omega_{He}$, where $\Omega_{He} = 9.97 \times 10^{-30}$ m^3 is the atomic volume of helium. The concentration of self-interstitials in local thermodynamic equilibrium with the bubble is then given by

$$C^o_I = \exp\{-\frac{(E^f_I + U_I)}{kT} + \frac{z(y_o)y_o\Omega}{\Omega_{He}} - \frac{2\gamma\Omega}{RkT}\} . \qquad (2)$$

The self-interstitial emission prevails over the helium interstitial emission whenever $C^o_I > C^o_{He}$ or

$$E^f_I + U_I + \frac{2\gamma\Omega}{R} - kT\left(\frac{\Omega}{\Omega_{He}}\right) y_o z(y_o) < E^f_{He} + U_{He} - kT\mu_g(y_o) . \qquad (3)$$

In the above equations U_I and U_{He} represent the interaction energy of the self-interstitial and the helium interstitial with the bubble. If both are treated as isotropic inclusions in an elastically isotropic material then only the image interaction and the modulus interaction contribute to U_I and U_{He}. The nearest interstitial sites are at a distance of b/2 from the center of the atoms forming the bubble surface. At this distance, the image interaction[9] is estimated to be about 0.3 U^R where U^R is the strain energy associated with the point defect. The modulus interaction of the self-interstitial is given by

$$U^m = \frac{3}{8}\alpha^G\left(1 + \frac{b}{2R}\right)^{-6}\left(\frac{p}{\mu} - \frac{2\gamma}{R\mu}\right)^2 \qquad (4)$$

where α^G = -150 eV is the shear polarizability. For a bubble radius R = 4b, γ = 2 J/m^2 and p/μ = 0.2, we find $U^m \cong$ - 0.7 eV. Since the formation energy of a self-interstitial is nearly equal to its strain energy, i.e. $U^R \cong E^f_I$, a formation energy of 6 eV is reduced near the bubble surface to about 3.8 eV by the image and modulus interaction.

The strain energy of a helium interstitial with a relaxation volume[3] of 0.6 Ω is about 1 eV near the bubble surface. Hence, (E^f_{He} + U_{He}) is about 3.5 eV in Ni if no modulus interaction exists for the helium interstitial.

Assuming then that the formation energies of self-interstitials and helium interstitials are about equal near a bubble surface, the condition (3) can be written as

$$[(\Omega/\Omega_{He})y_o z - \mu_g] > 2\gamma\Omega/RkT \ . \qquad (5)$$

At 300 K, the factor $2\gamma\Omega/RkT$ is approximately equal to 70 b/R in Ni. Hence, for bubbles with 2 nm in diameter, the gas density in the bubble must exceed a packing fraction of about 0.85 or a helium to vacancy ratio of more than 0.7 according to recently developed equations of state for helium.[10] If the density of helium is lower, helium emission is favored over self-interstitial emission. However, for lower values of y_o, $z(y_o)$ is also lower, and both C^o_{He} and C^o_I become very small, so that the rate of emission of either self- or helium interstitials becomes negligible. We can therefore conclude that when self-interstitial emission becomes a feasible process it is also favored over helium emission.

The pressure required for bubble growth by self-interstitial emission may be estimated as follows. Suppose that the rate of helium generation or implantation is $\dot{P}_{He}$ (per metal atom and per second), and that there are already N_B helium bubbles per unit volume of average radius R. Let us further assume that a stationary condition has been reached such that each new helium atom generated or implanted will after some time be trapped at one of the already existing bubbles. In addition, the ratio of helium atoms to vacancies in the bubble, η, shall remain constant, and any newly acquired helium atom in a bubble induces the emission of a self-interstitial. It is then obvious that the following relationship is valid:

$$\dot{P}_{He} = \eta 4\pi R N_B D_I C^o_I \ . \qquad (6)$$

Here, $D_I = D^o_I \exp(-E^m_I/kT)$ is the self-interstitial diffusion coefficient and C^o_I is given by Eq. (2) which depends on $p\Omega$, the work done by the gas per self-interstitial emission. From Eqs. (6) and (2) we obtain by neglecting U_I

$$p\Omega = \frac{2\gamma\Omega}{R} + E^f_I + E^m_I + kT \ln \left[\frac{\dot{P}_{He}}{\eta 4\pi R N_B D^o_I}\right] . \qquad (7)$$

In evaluating Eq. (7), the materials parameters listed in Table 1 were employed. It is found that the overwhelming contribution to the work $p\Omega$ comes from the interstitial formation energy E^f_I. In contrast, the parameters N_B, $\dot{P}_{He}$, η, and T can be varied over large ranges without much change in the work required to emit an interstitial. This is seen from the results shown in Figs. 1 and 2. Here, the indicated band covers the values for $p\Omega$ when the helium generation rate is varied between 100 and 1000 appm/s, the bubble density between 10^{17} and 10^{19} cm^{-3}, and the temperature between 300 K and 900 K. Furthermore, the work is only weakly dependent on the bubble radius R.

3. LOOP PUNCHING

Instead of the emission of one interstitial at a time, it is possible that an entire interstitial platelet may be emitted. As shown by Trinkaus and Wolfer,[11] the least energy is expended when the dislocation loop radius is R. For sufficiently large loop radii, the loop energy is given by

$$E_L = \frac{\mu b^2}{2(1-\nu)} R\left[\ln \frac{R}{r_o} - 2\ln 2 - 1\right] + \pi R^2 \gamma_f \qquad (8)$$

for a faulted loop where r_o is the dislocation core radius.

For small loops, the above expression becomes invalid. Based on computer simulation results of small interstitial clusters, Trinkaus[12] proposes the following approximation for the energy of a small interstitial loop

$$E_{IC} = \frac{8\pi\mu R}{a_o} \ . \qquad (9)$$

In order to obtain a continuous dependence of the loop energy on its radius R, we have

TABLE 1
Materials Parameters for Nickel and Austenitic Stainless Steels

PARAMETER	SYMBOL	VALUE	UNIT
Lattice parameter	a_o	0.364	nm
Surface energy	γ	2	J/m^2
Stacking fault energy	γ_f	0.3	J/m^2
Shear modulus	μ	10^{11}	Pa
Poisson's ratio	ν	0.3	
Vacancy formation entropy	S_v^f	1.5	k
Vacancy formation energy	E_v^f	1.8	eV
Vacancy migration energy	E_v^m	1.1	eV
Interstitial formation energy	E_I^f	3-6	eV
Interstitial migration energy	E_I^m	0.2	eV
Pre-exponential factors			
for vacancy diffusion	D_v^o	0.0153	cm^2/s
for interstitial diffusion	D_I^o	0.001	cm^2/s
Bubble density	N_B	10^{17}-10^{19}	cm^{-3}

chosen the core radius r_o such that $E_{IC} \cong E_L$ at R = 10 b. This particular matching is accomplished with $r_o \cong 0.1$ b.

The work performed per metal atom emission is now given by

$$p\Omega = \frac{2\gamma\Omega}{R} + \frac{E_L\Omega}{(\pi R^2 b)} \qquad (10)$$

where E_L is either equal to E_{IC} when R < 10 b, or equal to E_L for larger loop radii. We note that for R < 10 b, Eq. (10) gives the simple relationship

$$p\Omega = \frac{(2\gamma + \mu b)\Omega}{R} \, . \qquad (11)$$

Figures 1 and 2 show the work expended per metal atom emission according to Eq. (10) as the lower dashed curves. It is seen that the

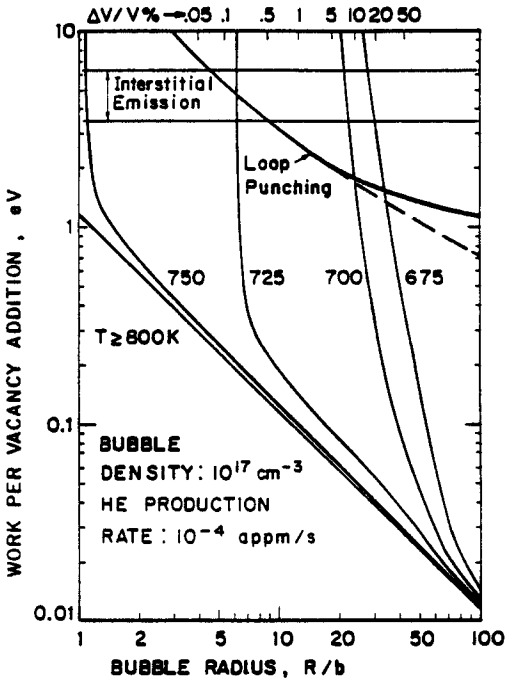

FIGURE 1
Energy expended per thermal vacancy absorption at a bubble. Case for helium production by transmutations.

loop punching mechanism requires less work per atom for bubble radii greater than 5 to 10 Burgers vectors when compared to the interstitial emission process.

The above condition for loop punching, first proposed by Greenwood et al.[8] is based on energy considerations which do not take into account both the image interaction of the loop with the bubble and the interaction with the stress field of the overpressurized bubble. When these interactions are included[11] it is found that an appreciable activation barrier exists for the expulsion of the loop, and the pressure required exceeds the one according to the condition of Eq. (11) when the loops have radii larger than about 20 b. These higher pressures give results indicated by the upper solid curves in Figs. 1 and

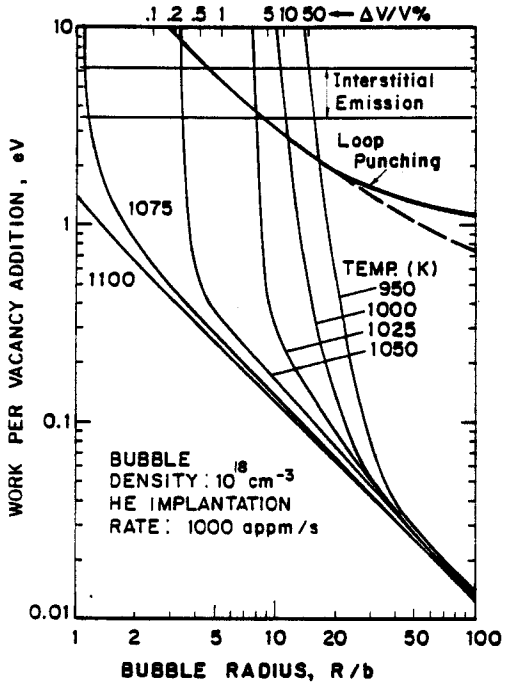

FIGURE 2
Same as Fig. 1, but for the case of helium implantation typical of blistering studies.

2, whereas Eq. (11) gives results indicated y the dashed curves.

4. THERMAL VACANCY ABSORPTION

The vacancy concentration in local thermodynamic equilibrium with a bubble is given by

$$C_v^o = C_v^{eq} \exp\left(+\frac{p_o\Omega}{kT}\right) \tag{12}$$

where

$$-p_o = p - \frac{2\gamma}{R} \tag{13}$$

and

$$C_v^{eq} = \exp\left[\frac{S_v^f}{k} - \frac{E_v^f}{kT}\right] . \tag{14}$$

If σ_H represents the hydrostatic stress in the matrix of the solid which contains the bubbles, then the vacancy concentration in local thermodynamic equilibrium with dislocations and grain boundaries is given by

$$C_v^d = C_v^{eq} \exp\left(\frac{\sigma_H\Omega}{kT}\right) . \tag{15}$$

An overpressure in the bubbles ($p_o < 0$) will cause a hydrostatic tension in the matrix. As shown elsewhere,[13] this hydrostatic stress is approximately given by

$$\sigma_H \cong -p_o S^2 \tag{16}$$

where S is the volume fraction of the bubbles. Due to the overpressure in bubbles, $C_v^d > C_v^{eq} > C_v^o$, and a thermal vacancy flux will be induced from dislocations and grain boundaries to the bubbles. Under stationary conditions, the rate of helium generation becomes equal to the rate of helium capture at bubbles. In turn, this rate is then also equal to the rate of vacancy absorption at bubbles. Hence

$$\dot{p}_{He} = \eta 4\pi R N_B D_v C_v^{eq} \times \left\{\exp\left(-\frac{p_o S^2\Omega}{kT}\right) - \exp\left(+\frac{p_o\Omega}{kT}\right)\right\} . \tag{17}$$

This equation can only be solved numerically for $p\Omega$. However, when $|p_o|\Omega/kT \ll 1$, we may expand the exponentials to first order and obtain

$$p\Omega \cong \frac{2\gamma\Omega}{R} + \frac{kT\dot{p}_{He}}{(1 + S^2)\eta 4\pi R N_B D_{SD}} \tag{18}$$

where $D_{SD} = D_v C_v^{eq}$ is the self-diffusion coefficient. On the other hand, when $(-p_o\Omega/kT) \gg 1$, we may neglect the second term in the brackets of Eq. (17), and we obtain the approximation

$$p\Omega \cong \frac{2\gamma\Omega}{R} + \left(\frac{kT}{S^2}\right) \ln\left[\frac{\dot{p}_{He}}{\eta 4\pi R N_B D_{SD}}\right] . \tag{19}$$

Equation (17) was solved numerically for $p\Omega$ as a function of the bubble radius R. The results are shown in Figs. 1 and 2. For a helium production rates typical of (n,α) transmutations in HFIR or future fusion reactors, the

results in Fig. 1 show that thermal vacancy absorption is the predominant mechanism of bubble growth for irradiation temperatures > 800 K. As the swelling due to bubble growth increases, however, the hydrostatic stress σ_H increases in the matrix, and vacancy emission at dislocations can occur at somewhat lower temperatures. Consider, for example, irradiation at 700 K. Initially, small helium clusters grow by interstitial emission until their diameter reaches about ~ 2 nm; then, further growth occurs most likely by loop punching until the bubble swelling reaches about 10%. From then on, bubble growth takes place by thermal vacancy emission at dislocations and absorption at the bubbles.

If the helium concentration increases at a rate of 1000 appm/s as in helium implantation studies for blistering, the transition from one growth mechanism to another occurs at higher temperatures, as shown in Fig. 2.

5. DISCUSSION

The present assessment of helium bubble growth mechanisms can only provide a qualitative picture in the form of "bubble growth maps" displayed in Figs. 1 and 2. These maps simply indicate the predominant mechanism of bubble growth for given conditions, such as temperature, helium generation or implantation rate, and bubble density. The most serious drawback of these maps is that bias-driven growth of bubbles is not considered. Therefore, the assessment applies only to cases where either the displacement damage is not significant or bias-driven void growth does not occur. An example of the former is the case of blistering studies, where the ratio of helium to displacement damage is about 1000 appmHe/dpa and the temperature is below the stage for vacancy migration. Examples for the latter case are materials which exhibit a very long incubation time for void swelling. For these materials, helium bubble formation by the above mechanisms is expected to occur in a fusion environment. Once the bubbles have grown to a critical size, bias-driven growth should become significant and void swelling commences.

REFERENCES

1. J.E. Inglesfield, J.B. Pendry, Phil. Mag. 34 (1976) 205.
2. W.D. Wilson, C.L. Bisson, Rad. Effects 19 (1973) 53.
3. W.D. Wilson and R.A. Johnson, "Interatomic Potentials and Simulation of Lattice Defects," Eds. C. Gehlen, J.R. Beeler, R.I. Jaffee, Plenum, NY, 1972, p. 375.
4. W.D. Wilson, M.I. Baskes, C.L. Bisson, Phys. Rev. B13 (1976), 2470.
5. W.D. Wilson, C.L. Bisson, M.I. Baskes, Phys. Rev. B24 (1981) 5616.
6. M.I. Baskes, R.H.J. Fastenau, P. Penning, L.M. Caspers, A. van Veen, J. Nucl. Matls. 102 (1981) 235.
7. J.H. Evans, J. Nucl. Matls. 68 (1977) 129; J. Nucl. Matls. 76 & 77 (1978) 228.
8. G.W. Greenwood, A.J.E. Foreman, D.E. Rimmer, J. Nucl. Matls. 4 (1959) 305.
9. W.G. Wolfer, L.K. Mansur, J. Nucl. Matls. 91 (1980) 265.
10. W.G. Wolfer, B.B. Glasgow, W.F. Wehner, H. Trinkaus, Procs. of the 3rd Top. Mtg. on Fusion Reactor Materials, Albuquerque, NM, Sept. 19-22, 1983.
11. H. Trinkaus and W.G. Wolfer, Procs. of the 3rd Top. Mtg. on Fusion Reactor Materials, Albuquerque, NM, Sept. 19-22, 1983.
12. H. Trinkaus, Rad. Effects 99, in print.
13. W.G. Wolfer, B.B. Glasgow, DAFS Quarterly Progress Report DOE/ER-0046/12, Feb. 1983, p. 155.